TU Delft

Delft University of Technology

Database building and interpolation for a safe flight envelope prediction system

Zhang, Ye; De Visser, Coen C.; Chu, Q. Ping

DOI
10.2514/6.2018-1635

Publication date
2018

Document Version
Accepted author manuscript

Published in
AIAA Information Systems-AIAA Infotech at Aerospace

Citation (APA)
Zhang, Y., De Visser, C. C., & Chu, Q. P. (2018). Database building and interpolation for a safe flight envelope prediction system. In *AIAA Information Systems-AIAA Infotech at Aerospace* (209989 ed.). Article AIAA 2018-1635 American Institute of Aeronautics and Astronautics Inc. (AIAA). https://doi.org/10.2514/6.2018-1635

Important note
To cite this publication, please use the final published version (if applicable).
Please check the document version above.

Copyright
Other than for strictly personal use, it is not permitted to download, forward or distribute the text or part of it, without the consent of the author(s) and/or copyright holder(s), unless the work is under an open content license such as Creative Commons.

Takedown policy
Please contact us and provide details if you believe this document breaches copyrights.
We will remove access to the work immediately and investigate your claim.

This work is downloaded from Delft University of Technology.
For technical reasons the number of authors shown on this cover page is limited to a maximum of 10.

Database Building and Interpolation for a Safe Flight Envelope Prediction System

Y. Zhang*, C.C. de Visser† and Q.P. Chu.‡
Delft University of Technology, Delft, 2629HS, The Netherlands.

This paper reports the latest progress in the development of a database-driven safe flight envelope prediction system. By building up a database containing safe flight envelopes of different damage and fault scenarios, the challenges associated with online flight envelope prediction can be circumvented. The database is designed for different flight conditions at which the flight envelopes are computed. Both longitudinal and lateral envelopes are computed via the level set method, which shows obvious shrinkage between damaged and undamaged aircraft. It is found that by interpolating between two retrieved envelopes in the database, more accurate results can be achieved.

I. Introduction

Safety is of paramount importance to aviation. Among all the contributors that could potentially lead to unsafe flight, aircraft loss-of-control (LOC) is a dominant reason for many aircraft accidents that have happened in the past few decades [1–3]. Endeavors to prevent LOC accidents have been made throughout years in various aspects [4, 5]. A direct indication of LOC accidents is the violation of the flight envelope [6], which defines the region where the aircraft can be safely operated. Active research can be found in the field of LOC prevention and recovery through safe flight envelope prediction and protection [7–10].

The flight envelope is determined by the aerodynamic and kinematic model of the aircraft as well as its control authority. Different ways of describing a safe flight envelope can be found in literature [8, 11–15], depending on the measurements and states that are of highest concern in terms of safety. Among these methods, reachability analysis computes the safe flight envelope in a set-valued fashion, which defines a set of states that will reach the target set within a certain time horizon given the current control authority [16]. In order to evaluate the possibility of aircraft maneuvering to and recovering from a safe region, this paper adopts the methods of computing flight envelopes based on reachability analysis [9, 17], and its numerical solution is given by the level set method [18, 19].

During normal flight, the envelopes are fixed and stored in a flight envelope protection system to indicate perfor-

*PhD Student, Control and Simulation Section, Faculty of Aerospace Engineering, Delft University of Technology; Kluyverweg 1, 2629HS, Delft, The Netherlands. AIAA Student Member
†Assistant Professor, Control and Simulation Section, Faculty of Aerospace Engineering, Delft University of Technology; Kluyverweg 1, 2629HS, Delft, The Netherlands. AIAA Member
‡Associate Professor, Control and Simulation Section, Faculty of Aerospace Engineering, Delft University of Technology; Kluyverweg 1, 2629HS, Delft, The Netherlands. AIAA Member

mance and structural limits of the current states [7]. Under abnormal conditions, however, the stability margin and control authority might suddenly change due to abrupt system failures and structural damage, which leads to a changed flight envelope. In such moments, the LOC incident might follow if the shrunken envelope is not protected and the aircraft finds itself outside the new safe boundary. Therefore, it is essential to obtain the changed flight envelope online as fast as possible to allow for effective upset recovery based on fault tolerant control. To circumvent the challenges of updating global model of the impaired aircraft and the high computational load of determing the envelope, a fast database-driven method is proposed in our research, which is reffered to as the "Database-driven safE Flight ENvelope preDiction system (DEFEND)." [20].

The general process of DEFEND is illustrated in Fig. 1, where the onboard system and off-line database is connected by an information retrieval process. When off-nominal events suddenly occur, it is highly desirable to first characterize the adverse conditions of the aircraft. The system identification module [21] will locally update the aircraft model with new measurements. After that, faults and failure of actuators and engines can be detected and evaluated by fault detection and isolation (FDI) systems [22–26]. In the case of structural damage, a well-trained classifier is used to find out the damage type and severity. During the information retrieval process, the database takes in the index number of the specific abnormal case detected and classified in the previous step and retrieves the corresponding safe flight envelope.

The high richness of the database is one important feature that we are aiming for. The more situations are included in the database, the more accurate information on envelopes can be retrieved to enhance the safety level of the aircraft. Nevertheless, the number of envelopes stored in the database are restricted by physical limitations of conducting experiments with damaged aircraft models [20]. Therefore, interpolation is always needed when the required safe flight envelopes can not be directly retrieved from the database. What is addressed in this paper is online interpolation between two envelopes stored in the database to achieve the requirement of both safety and accuracy. Interpolation is applied to envelopes of different states and damage classes to enhance the richness of the database. The resulting safe flight envelope will be used for onboard cockpit display and fault tolerant controller [27]. The main contribution of this paper is building a database of safe flight envelopes under several structural damage cases and improving the retrieval process through online interpolation between envelopes.

II. Data Collection and Management

A. Abnormal Case Study

In NASA's design of safety-critical systems for aircraft LOC prevention and recovery [3, 12], a preliminary set of 60 LOC test scenarios were developed based on the past accidents analysis and potential future LOC risks [28]. As listed in Table 1, the set contains scenarios involving four LOC precursors categories [3], and each category can

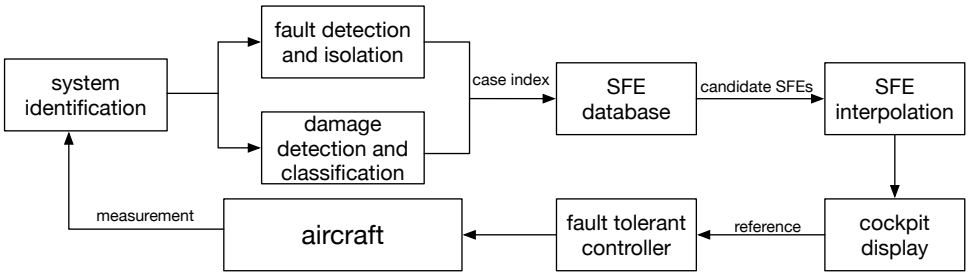

Fig. 1 General framework of database-driven safe flight envelope prediction system

be built for one database. This paper focuses on structural damage, which fundamentally changes the dynamics and control abilities of the aircraft and thus induces LOC accidents. The flight data of structural damaged aircraft can be generated by CFD/wind tunnel experiments [29] and be used by advanced system identification methods to determine their mathematical models. These models are used to calculate the safe flight envelopes for different flight situations. The building of the database is one of the key steps of proving the feasibility of the whole DEFEND system. Three major damage cases are considered in this paper, corresponding to safe flight envelopes in longitudinal and lateral motions.

Table 1 LOC Accidents Causal and Contributing Factors

System Faults and Failures	Strucutral Damage	External Hazards	Aircraft Upsets
jammed/ stuck control effector	wing tip loss	icing and snow	stall
actuator run away	engine loss	wind gusts	abnormal attitude
loss of control effectiveness	control surfaces damage	wake vortices	abnormal trajectory
engine failure	horizontal stabilizer tip loss	poor visibility	abnormal velocity
sensor faults	vertical tail tip loss	bird strike	

B. Safe Flight Envelope Calculation

Conventional flight envelopes mostly focus on indicating physical constraints on the aircraft without considering control goals. Despite the development of flight envelope protection systems, it may still be inadequate to help guarantee safety in unanticipated situations [30]. Therefore, it is necessary to synthesize control design in envelope prediction problems. Reachability analysis is chosen in this paper as the method to compute safe flight envelopes, since the theory provides a set-valued insight into safety and control design of dynamic systems. One advantage of this method is that all possible trajectories can be computed from all available control strategies and initial states, which naturally meets the safety guarantees [19]. The computed results are called reachable sets, which are defined as a set of states that reach a certain target set within given a certian time horizon and current control authority [16, 31]. The application of reachable sets in aircraft safety involves saving aircraft after the occurrence of unexpected incidents (e.g. system faults, structural damage). In such situations, the aircraft should firstly return to the safe trim set, and then maneuver

from the trim set to other possible flight conditions like landing. During the process, two reachable sets are needed, which are normally referred to as the backward reachable set and the forward reachable set [9, 27, 32], as displayed in Fig. 2. What we are looking for is the intersection between these two reachable sets of a given trim set, which indicates the region in the state space where aircraft can reach the trim set and maneuver freely within a certain time horizon.

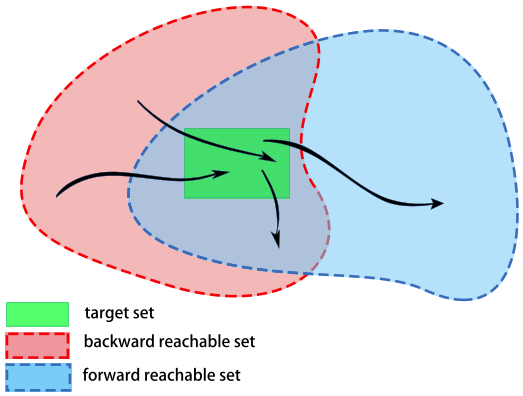

Fig. 2 Illustration of the safe flight envelope based on reachability analysis[20]

The boundary of reachable sets can be determined by solving for a value function and obtaining its zero level set [16]. A characterization of the value function as the viscosity solution to a time-dependent Hamilton-Jacobi-Isaacs (HJI) partial differential equation has been proposed and well developed, which is the key theory to solving reachability problems [16]. Several numerical techniques have been proposed to compute the viscosity solution to the HJI equation. In this paper we use the one developed by Osher and Sethian [33, 34] and is called the level set method, which has been successfully applied to the reachability analysis of many systems including aircraft. For more mathematical details, the reader can refer to Refs.[16, 33–35].

In this paper, the nonlinear model of a Cessna Citation is used to generate safe flight envelopes for the database. To compute reachable sets, the target set must be determined first, which is usually described by a signed distance function. In this paper, the target set is determined by the trim set, which is estimated by minimizing the cost function of model states [27].

Because of the 'curse of dimensionality' of the level set method, computing high-dimensional safe flight envelope is very time consuming. Thus in this paper, the dynamics of the aircraft are decoupled into longitudinal and lateral motions [16, 36–38]. Along each decoupled direction, three-dimensional safe flight envelopes are computed. Different combinations of states lead to different shapes of safe flight envelopes, which can be stored and selected by pilots. It is important to note that aircraft stall is not the scope of this paper, since the aerodynamic model of high angle of attack regime is highly nonlinear, which requires further modeling work before a safe flight envelope can be determined. For the primary phase of the research, we first compute safe flight envelopes of one category in Table 1, which is

in-flight structural damage. It is assumed that the structural damage discussed in this paper is not catastrophic and is still recoverable. Considering the infinite number of potential damage locations on an aircraft, this paper only focus on damage with significant controllability effects, like tip loss of wings and tails [29]. The intrinsic impact of structural damage is the change of aerodynamic characteristics of the aircraft [29, 39], which is directly reflected in the altered mathematical aerodynamic model both in its structure and parameters [24].

In this paper, three sets of envelopes are computed. One is the pitching envelope in longitudinal motion under horizontal tail damage. The other two in lateral motion are the yawing envelope under vertical tail damage and the rolling envelope under wing tip loss. It will be shown in the following examples that the computed envelopes under damage cases will shrink from their original damage-free shape. Based on these examples, we can generate a complete offline database containing different abnormal scenarios.

1. The Nonlinear Aircraft Model

The model that is used in envelope computation is based on the flat-earth kinematic and moment equations in body axes and the flat-earth force equations in wind axes. The kinematic equations, which do not depend on the aerodynamic model of the aircraft, are not influenced by structural damage [40]:

$$\begin{aligned} \dot{\phi} &= p + \tan\theta(q\sin\phi + r\cos\phi) \\ \dot{\theta} &= q\cos\phi - r\sin\phi \\ \dot{\psi} &= \frac{q\sin\phi + r\cos\phi}{\cos\theta} \end{aligned} \tag{1}$$

The equations of motion, on the other hand, are significantly affected by structural damage due to the change of moments and mass properties [40]:

$$\begin{aligned} \dot{p} &= (c_1 r + c_2 p)q + c_3(\tfrac{1}{2}\rho V^2 SbC_l) + c_4(\tfrac{1}{2}\rho V^2 SbC_n) \\ \dot{q} &= c_5 pr - c_6(p^2 - r^2) + c_7(\tfrac{1}{2}\rho V^2 SbC_m) \\ \dot{r} &= (c_8 p + c_2 r)q + c_4(\tfrac{1}{2}\rho V^2 SbC_l) + c_9(\tfrac{1}{2}\rho V^2 SbC_n) \end{aligned} \tag{2}$$

where $c_1 - c_9$ are combinations of moments and cross-productions of inertia derived from the inverse of the inertia matrix [40]. The effects of structural damage on mass properties have been investigated in wing tunnel experiments [41], and it is concluded that the effects of mass property changes are not significant compared with that of aerodynamic changes induced by aerodynamic surface lose. Therefore, in this paper, properties like aircraft mass, centers of gravity and inertia matrix are assumed unchanged after structural damage. The wind-axes force equations transformed from

body axes are [40]:

$$\begin{aligned}
\dot{V} &= \tfrac{1}{m}\left(T\cos\alpha\cos\beta - \tfrac{1}{2}\rho V^2 S C_D + mg_1\right) \\
\dot{\beta} &= \tfrac{1}{mV}\left(-T\cos\alpha\sin\beta + \tfrac{1}{2}\rho V^2 S C_Y - mVr_w + mg_2\right) \\
\dot{\alpha} &= \tfrac{1}{mV\cos\beta}\left(-T\sin\alpha\cos\beta - \tfrac{1}{2}\rho V^2 S C_L - mVq_w + mg_3\right)
\end{aligned} \tag{3}$$

where r_w and q_w are two components of rotational rates $[p_w, q_w, r_w]$ along the wind axes, which are transformed from rotational rates in body axes $[p, q, r]$ by [40]:

$$\begin{bmatrix} p_w \\ q_w \\ r_w \end{bmatrix} = \begin{bmatrix} \cos\alpha\cos\beta & \sin\beta & \sin\alpha\cos\beta \\ -\cos\alpha\sin\beta & \cos\beta & -\sin\alpha\sin\beta \\ -\sin\alpha & 0 & \cos\alpha \end{bmatrix} \begin{bmatrix} p \\ q \\ r \end{bmatrix} \tag{4}$$

and the components of the gravity vector are given by [40]:

$$\begin{aligned}
g_1 &= g(-\cos\alpha\cos\beta\sin\theta + \sin\beta\sin\phi\cos\theta + \sin\alpha\cos\beta\cos\phi\cos\theta) \\
g_2 &= g(\cos\alpha\sin\beta\sin\theta + \cos\beta\sin\phi\cos\beta - \sin\alpha\sin\beta\cos\phi\cos\theta) \\
g_3 &= g(\sin\alpha\sin\theta + \cos\alpha\cos\phi\cos\theta)
\end{aligned} \tag{5}$$

The aerodynamic model of the undamaged Cessna Citation aircraft used in this paper is [20]:

$$\begin{aligned}
C_D &= C_{D_0} + C_{D_\alpha}\alpha + C_{D_{\alpha^2}}\alpha^2 + C_{D_q}\frac{q\bar{c}}{V} + C_{D_{\delta_e}}\delta_e \\
C_Y &= C_{Y_0} + C_{Y_\beta}\beta + C_{Y_p}\frac{pb}{2V} + C_{Y_r}\frac{rb}{2V} + C_{Y_{\delta_a}}\delta_a + C_{Y_{\delta_r}}\delta_r \\
C_L &= C_{L_0} + C_{L_\alpha}\alpha + C_{L_q}\frac{q\bar{c}}{V} + C_{L_{\delta_e}}\delta_e \\
C_l &= C_{l_0} + C_{l_\beta}\beta + C_{l_p}\frac{pb}{2V} + C_{l_r}\frac{rb}{2V} + C_{l_{\delta_a}}\delta_a + C_{l_{\delta_r}}\delta_r \\
C_m &= C_{m_0} + C_{m_\alpha}\alpha + C_{m_q}\frac{q\bar{c}}{V} + C_{m_{\delta_e}}\delta_e \\
C_n &= C_{n_0} + C_{n_\beta}\beta + C_{n_p}\frac{pb}{2V} + C_{n_r}\frac{rb}{2V} + C_{n_{\delta_a}}\delta_a + C_{n_{\delta_r}}\delta_r
\end{aligned} \tag{6}$$

The aerodynamic characteristics of a structurally damaged aircraft has been investigated through a series of flight tests [42], wind-tunnel and computational experiments [29, 39, 41, 43] conducted by NASA. In these experiments, the damage was modeled in the form of partial or complete tip loss of major aerodynamic surfaces like horizontal stabilizers, vertical tail, and wings. The experiments are conducted on a 5.5% geometrically and dynamically scaled model of a generic transport airplane, which is referred to as the Generic Transport Model (GTM) [42]. The resulting aerodynamic model of the damaged aircraft in the form of look-up tables can be found in an open-source simulation

software [44]. Also, preliminary work on damage modeling of a Cessna Citation aircraft was performed in our group using digital DATCOM with various levels of vertical tail damage [45]. By analyzing these experimental data, it is observed that damage to different aerodynamic surfaces results in unique aerodynamic effects, which is reflected in the changes of different stability and control derivatives. More importantly, the changed aerodynamic coefficients can be modeled by multiplying the original value with a scaling factor. In some cases like wing damage, an incremental term as a function of flight states is added to the original model due to the induced asymmetry. Similar ways of damage modeling can be found in [46, 47], where the models of aircraft with wing damage is incorporated in the flight control design. In this paper, the model of a structurally damaged Cessna Citation aircraft is built on the data and observations of aforementioned experiments.

2. Longitudinal Envelopes

Under the condition of zero yaw rate $r = 0$ and zero sideslip angle $\beta = 0$, the resulting dynamics from Eq. 1- 5 can be written as:

$$\begin{aligned}
\dot{V} &= \tfrac{1}{m}\left[T\cos\alpha - \tfrac{1}{2}\rho V^2 S C_D + mg(-\cos\alpha\sin\theta + \sin\alpha\cos\phi\cos\theta)\right] \\
\dot{\alpha} &= -\tfrac{1}{mV}\left[T\sin\alpha + \tfrac{1}{2}\rho V^2 S C_L - mg(\sin\alpha\sin\theta + \cos\alpha\cos\phi\cos\theta)\right] + q \\
\dot{\theta} &= q\cos\phi \\
\dot{\phi} &= p + q\tan\theta\sin\phi \\
\dot{p} &= \frac{1}{(J_{xx}J_{zz} - J_{zx}^2)}\left[(J_{xx} - J_{yy} + J_{zz})J_{xz}pq + \tfrac{1}{2}\rho V^2 S b(J_{zz}C_l + J_{zx}C_n)\right] \\
\dot{q} &= \tfrac{1}{2}\rho V^2 S c\frac{C_m}{I_{yy}} - \frac{J_{xz}}{J_{yy}}p^2
\end{aligned} \tag{7}$$

By assuming constant velocity and roll angle, a three-dimensional pitch envelope of (α, θ, q) can be computed based on the simplified model. Figure 3 shows the safe flight envelops computed from Eq. 7 at sea level with states $(\alpha, \theta, q, V = 100m/s)$ and time horizon $T = 1s$. The control inputs are thrust and elevator deflections. Figure 3(a) shows both forward and backward reachable sets, which form the safe flight envelope displayed in Fig. 3(b) by taking the intersection between them. If one of the horizontal tails is damaged, the mostly influenced is pitching moment coefficient C_m, which is modeled as:

$$C_{m_{dmg}} = (1 + \lambda_m)C_m \tag{8}$$

where the damage scale λ_m is derived from experimental data. Besides, the pitch control power will reduce due to the damaged elevator. Figure 3(c) and (d) show how the envelopes reduce with horizontal stabilizer damage under the same condition. The shrinkage is shown in a more straightforward way in Fig. 4 by projecting 3D shapes into 2D contours with specific values of the third states.

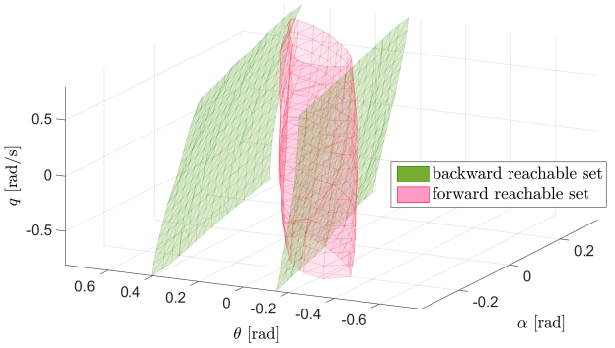

(a) Two reachable sets without damage

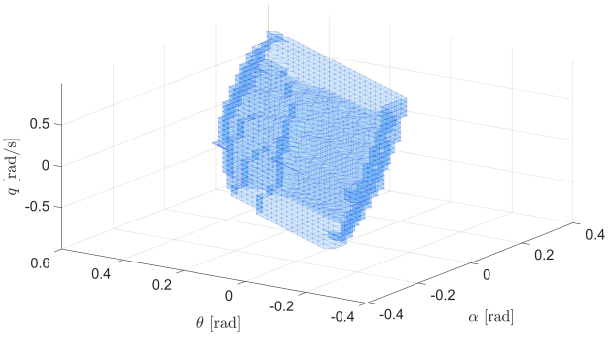

(b) Safe flight envelope without damage

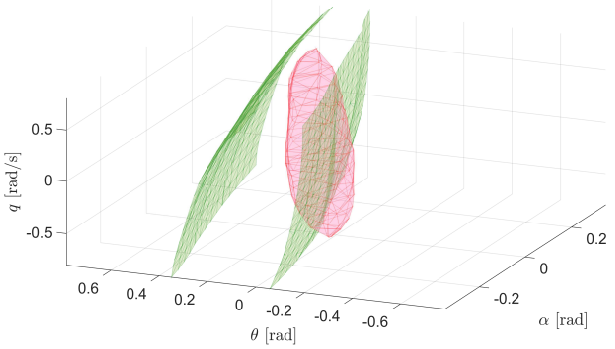

(c) Two reachable sets with damage

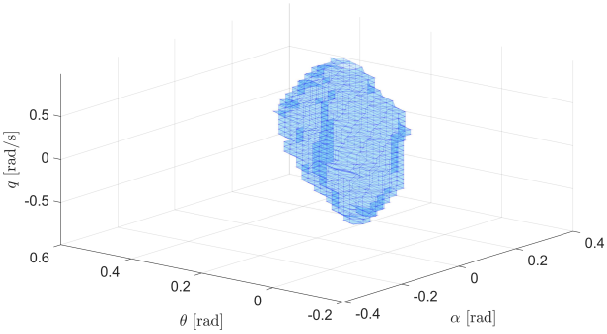

(d) Safe flight envelope with damage

Fig. 3 Comparison of (α, θ, q) envelopes under 30% horizontal stabilizer damage

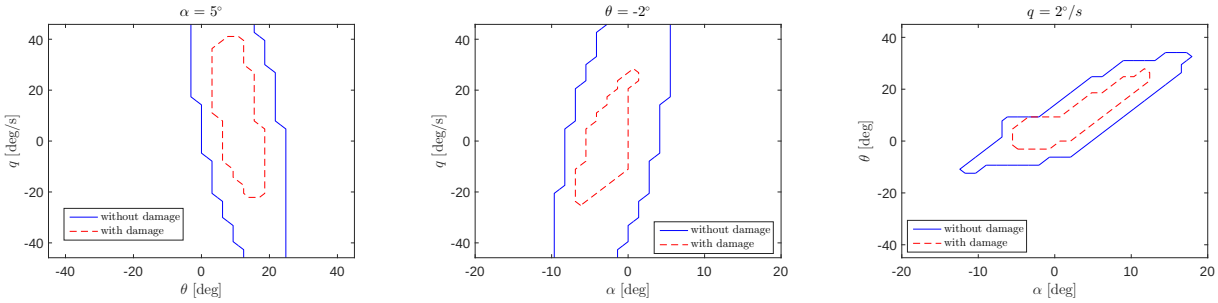

(a) (b) (c)

Fig. 4 2D-projected (α, θ, q) envelopes with and without 30% horizontal tail damage

3. Lateral Envelopes

The lateral motion of aircraft with zero pitch rate $q = 0$ is defined as [40, 48]:

$$\begin{aligned}
\dot{\beta} &= p\sin\alpha - r\cos\alpha + \tfrac{1}{mV}\left(-T\cos\alpha\sin\beta + \tfrac{1}{2}\rho V^2 S C_Y + mg_2\right) \\
\dot{r} &= \frac{1}{2(J_{xx}J_{zz} - J_{zx}^2)}\rho V^2 Sb(J_{zx}C_l + J_{xx}C_n) \\
\dot{p} &= \frac{1}{2(J_{xx}J_{zz} - J_{zx}^2)}\rho V^2 Sb(J_{zz}C_l + J_{zx}C_n) \\
\dot{\psi} &= r\frac{\cos\phi}{\cos\theta} \\
\dot{\phi} &= p + r\tan\theta\cos\phi
\end{aligned} \tag{9}$$

The yaw envelopes of time horizon $T = 1s$ are computed with states (β, r, ψ) when $\dot{p} = p = \dot{\phi} = \phi = 0$, which are shown in Figs. 5 and 6. The control inputs are thrust and rudder deflections. The changed yawing moment and reduction in directional stability due to vertical tail and rudder damage is modeled as:

$$C_{n_{dmg}} = (1 + \lambda_n)C_n \tag{10}$$

Based on this model, the reduction of the yawing envelope is observed.

The rolling envelopes shown in Figs. 7 and 8 are computed on the assumption of zero yaw rate ($\dot{r} = r = 0$). The control input are thrust and aileron deflections. For wing damage, an incremental rolling moment ΔC_l that increase with α is added to the baseline model along with the change of stability and control derivatives in Eq. 6:

$$C_{l_{dmg}} = (1 + \lambda_l)C_l + \Delta C_{l_\alpha}\alpha \tag{11}$$

The parameters of the damaged model are approximated and identified from experimental data. Besides, available roll control power is reduced due to structural damage and part of the aileron control is used to compensate for roll asymmetry. The restricted rolling maneuvers of p and ϕ are observed in Figs. 7 and 8.

III. Information Retrieval and Interpolation

A. Database Design and Structure

Based on the computed safe flight envelopes, a database containing offline calculated envelopes under different fault and damage scenarios can be designed and established. Table 2 shows the main attributes that should be included in the database. For each category only a few examples are listed for demonstration, which shows how much information needs to be specified in order to retrieve an envelope in the database. It is noted that the envelopes corresponding

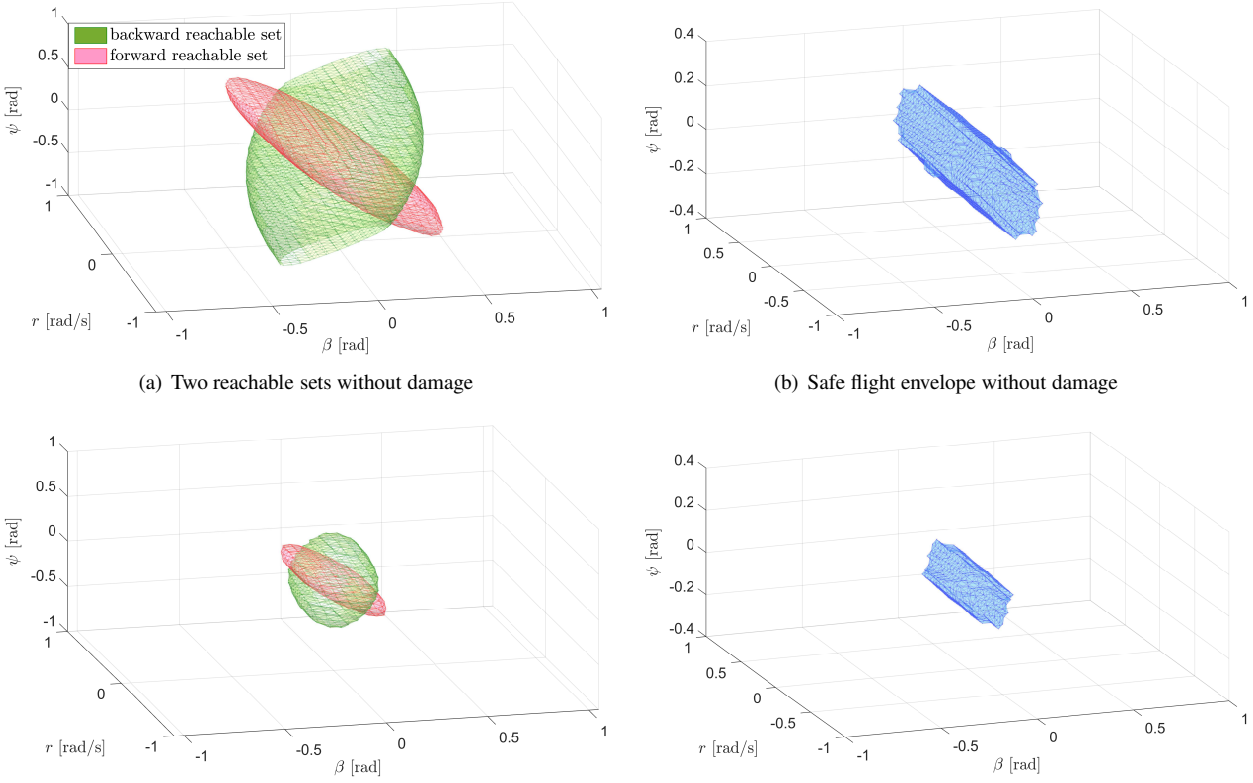

(a) Two reachable sets without damage

(b) Safe flight envelope without damage

(c) Two reachable sets with damage

(d) Safe flight envelope with damage

Fig. 5 Comparison of (β, r, ψ) envelopes with and without 40% vertical tail damage

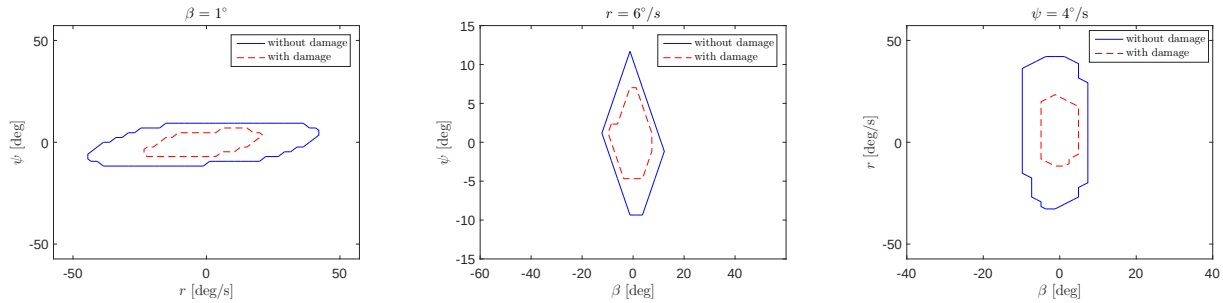

(a) (b) (c)

Fig. 6 2D projected (β, r, ψ) envelopes with and without 40% vertical tail damage

to actuators damage (elevator, rudder, ailerons) are not shown in this paper though listed in the table. This is because the damage to actuators is less severe case compared with damage to large aerodynamic surfaces, and the envelopes of the damage share similar trends in each individual channel.

B. Information Retrieval with Safety Considerations

Once the database is successfully built, the next thing is to ensure that the information can be retrieved in a correct and efficient way. Among all the attributes that determine one safe flight envelope in the database, the most important

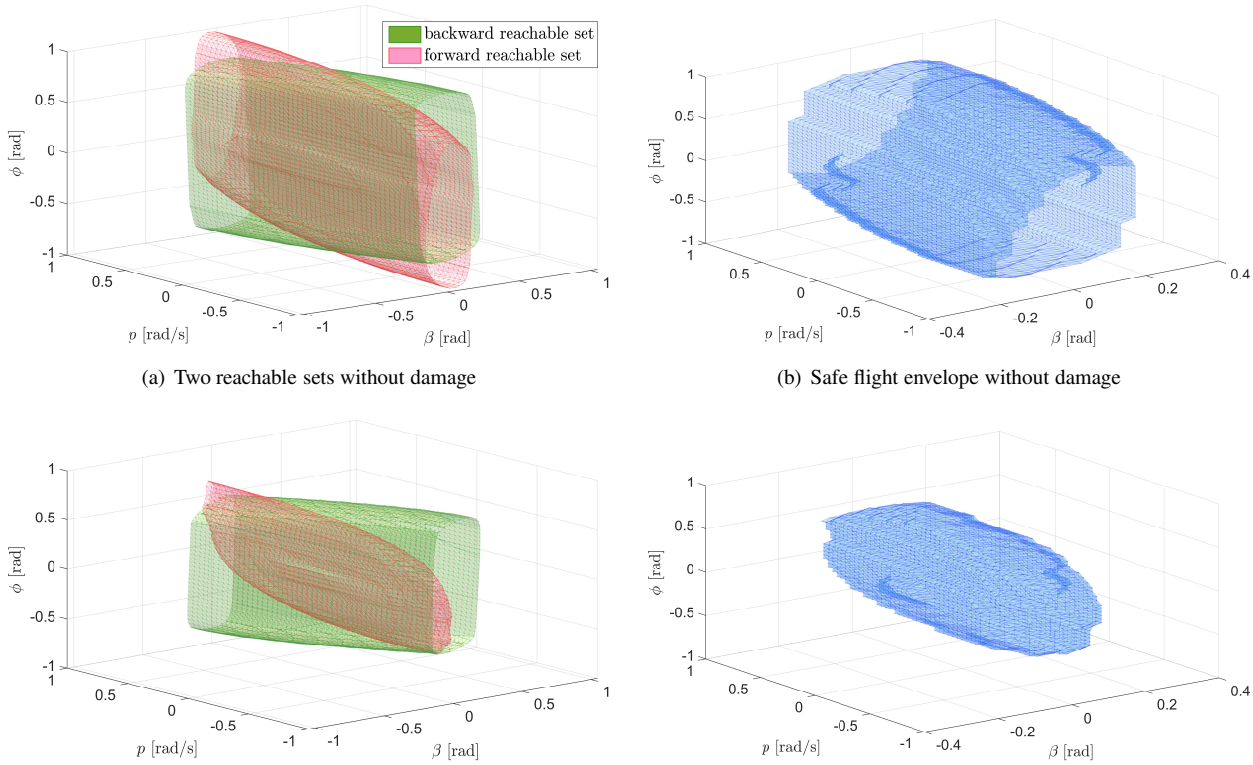

(a) Two reachable sets without damage

(b) Safe flight envelope without damage

(c) Two reachable sets with damage

(d) Safe flight envelope with damage

Fig. 7 Comparison of (β, p, ϕ) envelopes with and without 20% wing damage

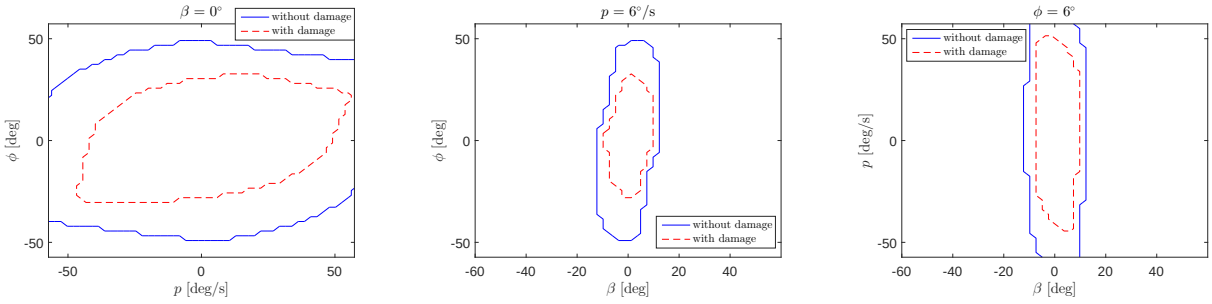

(a) (b) (c)

Fig. 8 2D projected (β, p, ϕ) envelopes with and without 20% wing damage

ones are specified by the first three columns in Table 2, which are found through classification methods. The pre-defined class labels for classification conform to the ones listed in the database. The identified aerodynamic coefficients are used as input features to the classifier. Further details on damage classification can be found in Ref. [20]. In real applications, safety should be included as the primary consideration. Since the finite number of safe flight envelopes in the database is accordance with the number of abnormal cases and discrete flight states, there always are situations where the true, unknown flight envelope falls in between the two neighboring categories in the database. In order to obtain more accurate results from the database, interpolation between two envelopes is necessary [20]. Generally,

Table 2 Preliminary Design of Safe Flight Envelope Database

Location	Type	Severity	Time	Model	Mach	Altitude
right horizontal stabilizer	tip loss	30%	$1s$	(α, q, θ)	0.3	sea level
	tip loss	50%	$2s$	(α, q, θ)	0.4	5000
elevator	stuck	15°	$1s$	(α, q, θ)	0.3	10000
	loss of effectiveness	30%	$2s$	(α, q, θ)	0.4	5000
left wing	tip loss	40%	$1s$	(β, p, ϕ)	0.5	sea level
	tip loss	60%	$2s$	(β, p, ϕ)	0.6	5000
vertical tail	tip loss	20%	$1s$	(β, r, ψ)	0.8	10000
	tip loss	40%	$2s$	(β, r, ψ)	0.6	5000

interpolation is implemented with respect to two entities in the database. The first one includes the flight states and time horizons, e.g., envelopes of two different values of airspeed or altitude. The second entity is related to the specific condition of damage and failures. Take wing damage for example, if the current percentage of tip loss is estimated as 10% but only envelopes of 20% are available in the database. In this situation, interpolation between envelopes of no damage and 20% wing tip loss is needed to acquire the envelope corresponding to the estimated 10% damage.

C. Safe Flight Envelope Interpolation

For two envelopes computed by the level set method, the idea is to simply treat them as two different implicit functions. The method used for interpolation in this paper is inspired by research on surface reconstruction and image matching using the level set method and fast marching method [49–52]. In [49], an efficient algorithm is applied to approximate surfaces consisting of data points by constructing and driving a distance function. The concept of the distance function is also found in the fast marching method proposed in [53], which is an efficient way of propagating and tracking implicit fronts. The method of interpolation used in this paper is composed of three steps. The first step is to transform envelopes into a set of data points based on the characteristic of implicit functions. The second step is to find the geometric relationship between the two envelopes by finding out the distance function that matches one to another using the fast marching method [53]. The third step is interpolation between two envelopes based on their geometric relationship.

1. Envelopes Represented by Data Points

As introduced in Sec. B, the safe flight envelope is a set-valued result of an optimal-control based reachability problem. The resulting reachable set is represented as the zero-level set of an implicit surface function ϕ. Without an explicit analytic expression, the surface function is approximated by values in grid points, which are propagated from an initial set in a certain velocity field. Therefore, the envelope can be approximated by points on the zero level boundary or points lying around the boundary. Given a grid point $C(i, j)$ and its three neighboring points, if their

function values satisfy [54]:

$$\max(\phi_{i,j}, \phi_{i+1,j}, \phi_{i,j+1}, \phi_{i+1,j+1}) < 0 \qquad \text{OR} \qquad \min(\phi_{i,j}, \phi_{i+1,j}, \phi_{i,j+1}, \phi_{i+1,j+1}) > 0 \tag{12}$$

then $C(i, j)$ doesn't belong to the surface that represents the envelope and is ignored, else, it will be stored as part of the data set that approximates the zero level set. In this way, the retrieved envelopes can be approximated by the data points, which will be used to compute interpolation path between them.

2. Optimal Path Planing Based on the Fast Marching Method

The key step to be taken before interpolation is to find the relationship between two envelopes through surface mapping. Since the retrieved envelopes calculated from different models have been discretized into data points, only a geometrical mapping is investigated instead of mapping two implicit functions. For simplicity and a proof of concept, only two-dimensional envelopes are investigated in this paper, since a three-dimensional envelope can be projected into a $2D$ plane. The extension to three-dimensional surface will be included in future work. In this cases, two contours are treated as two sets of data points, and the mapping is implemented pair-wise by finding the optimal path between two points. Given a cost function F and a staring point A, the goal in path planing is to construct the path $\gamma(\tau)$ from A to destination point B that minimizes the integral. In two dimentsions, let T be the minimal cost required to travel from A to the point (x, y), that is [53],

$$T(x, y) = \min_{\gamma} \int_{A}^{(x,y)} F(\gamma(\tau))d\tau \tag{13}$$

where τ is the arclength parameterization of γ, namely, $|\gamma_\tau| = 1$. The level set $T(x, y) = c$ is the set of all points that can be reached with minimal cost c, and the minimal cost paths are orthogonal to the level curves; hence we have

$$|\nabla T| = F(x, y) \tag{14}$$

which forms an Eikonal equation [53]. The fast marching method provides a numerical scheme for computing solution to the Eikonal equation based on entropy-satisfying upwind schemes and fast sorting techniques [53]. Readers can refer to Refs. [50, 51, 53] for more details. Once solution $T(x, y)$ is computed, the shortest path can be constructed through back-propagation from destination point B via solving the ordinary differential equation:

$$X_t = -\nabla T \qquad \text{given } X(0) = B \tag{15}$$

until the staring point A is reached [53]. In this paper, the cost function F is set to be 1.

3. Envelope Interpolation

Linear interpolation can be implemented on each optimal path between data points of the two envelopes. It is assumed that the points that form the interpolated contour also lie on the optimal path, and their specific locations along the path are determined by the interpolation weights. These weights are heuristically chosen based on different conditions in which the envelopes are computed. The interpolation of the database in our research is initiated by a safety-related problem [20]. In the database, the number of stored safe flight envelopes for different abnormal cases is limited. Take structural damage for example, the closer the discrete values of damage levels are to each other, the more accurately the true safe flight envelopes can be predicted. However, the number of designed damage levels is restricted by physical limitations of modeling experiments like wind-tunnel tests and simulations. Therefore, when it is required to retrieve a safe flight envelope in between two stored envelopes in the database, a safer approach would be through interpolation rather than taking either side when the interval is too large.

In Fig. 9, the lateral envelopes under wing damage are used as the first example for demonstration. Figure. 9(a) shows three 2D envelopes in (p, ϕ) computed by the level set method. The largest contour is computed without any damage and the smallest one is computed with 20% wing tip loss. The contour in between them corresponds to the envelope of 10% tip loss, which is used and displayed to test the performance of the interpolation with the method proposed in this section. The envelopes of zero damage and 20% damage are approximated and transformed to data points (fig. 9(b)) based on Eq. 12. Then, optimal paths between the points on the largest and the smallest contour are computed, which are represented in yellow dashed lines in fig. 9(b). After the mapping is built between two envelopes, linear interpolation is performed to find the points on the optimal path that approximate the intermediate envelope, which is shown in 9(b). It can be observed in fig. 9(c) that the interpolated contour accurately approximates the true envelope of 10% wing damage.

Damage level is not the only decisive factor in the database. Some other entities, like velocity, altitude and time horizon are also important in building the database. As shown in Table. 2, the value of these entities are also discrete, which means that interpolation is necessary when specific values of certain states are required. The second example demonstrated in Fig. 10 deals with envelopes of different velocities. Figure. 10(a) shows three 2D envelopes in (β, r) computed by the level set method. The inner and outer envelopes correspond to $V = 60m/s$ and $V = 100m/s$ respectively. The task is to find out the contour of $V = 80m/s$ by interpolating between the two known contours. Following the similar steps of fast marching method used in the first example, the intermediate contour is found, which approximates the true contour with satisfying accuracy, as shown in Fig. 10(c).

IV. Conclusion

This paper discusses the implementation of database building and interpolation for the online database-driven safe flight envelope prediction system. Envelopes in both longitudinal and lateral motions are computed by the level set

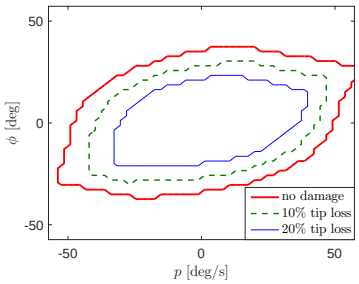

(a) Two-dimensional (p, ϕ) envelopes computed by the level set method

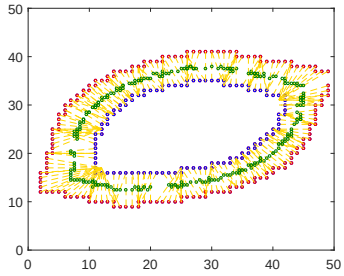

(b) Computed optimal paths and the resulting interpolated contour

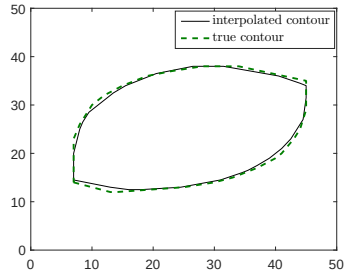

(c) Comparison between the interpolated contour and the true contour of 10% wing damage

Fig. 9 Interpolation between envelopes of different damage levels based on the fast marching method

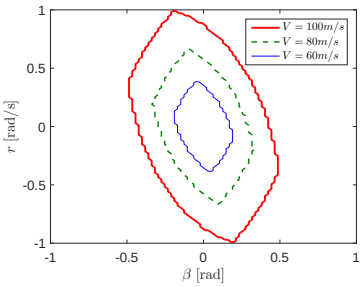

(a) Two-dimensional (β, r) envelopes computed by the level set method

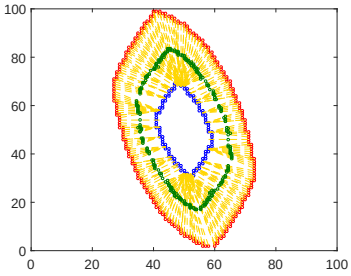

(b) Computed optimal paths and the resulting interpolated contour

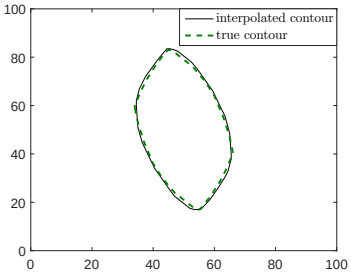

(c) Comparison between the interpolated contour and the true contour of $V = 80m/s$

Fig. 10 Interpolation between envelopes of different velocities based on the fast marching method

method, which shows obvious shrinkage with the occurrence of model change due to structural damage. The database is built with envelopes of different flight conditions and abnormal cases. In order to address the potential safety issue brought by the insufficient number of envelopes stored in the database due to limitations of damage modeling experiments, interpolation is implemented between 2-dimensional envelopes using the fast marching method. An example on wing damage shows the necessity of the interpolation, and the intermediate envelope computed by the interpolation algorithm shows satisfactory results.

References

[1] Ranter, H., "Airliner Accident Statistics 2006," Tech. rep., Aviation Safety Network, 2007.

[2] Company, B., "Statistical Summary of Commercial Jet Airplane Accidents: Worldwide Operations since 1959." Tech. rep., Boeing Commercial Airplanes, 2009.

[3] Belcastro, C. M., "Validation of Safety-Critical Systems for Aircraft Loss-of-Control Prevention and Recovery," *AIAA Guidance Navigation and Control Conference*, 2012.

[4] Belcastro, C. M., Foster, J. V., Newman, R. L., Groff, L., Crider, D. A., and Klyde, D. H., "Aircraft Loss of Control: Problem

Analysis for the Development and Validation of Technology Solutions," *AIAA Guidance, Navigation, and Control Conference*, 2016. doi:10.2514/6.2016-0092, URL http://arc.aiaa.org/doi/10.2514/6.2016-0092.

[5] Belcastro, C. M., Foster, J. V., Shah, G. H., Gregory, I. M., Cox, D. E., Crider, D. A., Groff, L., Newman, R. L., and Klyde, D. H., "Aircraft Loss of Control Problem Analysis and Research Toward a Holistic Solution," *Journal of Guidance, Control, and Dynamics*, Vol. 40, No. 4, 2017, pp. 733–775. doi:10.2514/1.G002815, URL https://arc.aiaa.org/doi/10.2514/1.G002815.

[6] Russell P., P. J., "Joint Safety Analysis Team- CAST Approved Final Report Loss of Control JSAT Results and Analysis," Tech. rep., Federal Aviation Administration: Commercial Airline Safety Team, 2000.

[7] Chongvisal, J., and Talleur, D., "Loss-of-control Prediction and Prevention for NASA's Transport Class Model," *AIAA Guidance, Navigation, and Control Conference*, 2014. URL http://arc.aiaa.org/doi/pdf/10.2514/6.2014-0784.

[8] Govindarajan, N., "An Optimal Control Approach for Estimating Aircraft Command Margins," Ph.D. thesis, 2012.

[9] Van Oort, E. R., "Adaptive Backstepping Control And Safety Analysis For Modern Fighter Aircraft," Ph.D. thesis, 2011.

[10] Wilborn, J., and Foster, J., "Defining Commercial Transport Loss-of-control: A Quantitative Approach," *AIAA Atmospheric Flight Mechanics Conference*, 2004. URL http://arc.aiaa.org/doi/pdf/10.2514/6.2004-4811.

[11] Tang, L., Roemer, M., Ge, J., Prasad, J., and Belcastro, C., "Methodologies for Adaptive Flight Envelope Estimation and Protection," *AIAA Guidance, Navigation and Control Conference*, 2009.

[12] Belcastro, C. M., "Validation and Verification of Future Integrated Safety-critical Systems Operating Under Off-nominal Conditions," *AIAA Guidance, Navigation, and Control Conference*, 2010. URL http://arc.aiaa.org/doi/pdf/10.2514/6.2010-8143.

[13] Kwatny, H. G., Dongmo, J.-E. T., Chang, B.-C., Bajpai, G., Yasar, M., and Belcastro, C. M., "Aircraft Accident Prevention : Loss-of-Control Analysis," *AIAA Guidance Navigation and Control Conference*, 2009. doi:10.2514/6.2009-6256, URL http://www.pages.drexel.edu/{~}hgk22/papers/AIAA-2009-6256-834.pdf.

[14] Kwatny, H. G., Dongmo, J.-E. T., Allen, R. C., Chang, B.-C., and Bajpai, G., "Loss-of-Control: Perspectives on Flight Dynamics and Control of Impaired Aircraft," *AIAA Guidance, Navigation, and Control Conference*, 2010. doi:10.2514/6.2010-8005, URL http://arc.aiaa.org/doi/abs/10.2514/6.2010-8005.

[15] Kwatny, H. G., Dongmo, J.-E. T., Chang, B.-C., Bajpai, G., Yasar, M., and Belcastro, C. M., "Nonlinear Analysis of Aircraft Loss of Control," *Journal of Guidance, Control, and Dynamics*, Vol. 36, No. 1, 2013, pp. 149–162. doi:10.2514/1.56948, URL http://arc.aiaa.org/doi/abs/10.2514/1.56948.

[16] Lygeros, J., "On Reachability and Minimum Cost Optimal Control," *Automatica*, Vol. 40, 2004, pp. 917–927. URL http://www.sciencedirect.com/science/article/pii/S0005109804000263.

[17] Lombaerts, T., and Schuet, S., "Robust Maneuvering Envelope Estimation Based on Reachability Analysis in An Optimal Control Formulation," *Conference on Control and Fault-Tolerant System*, 2013, pp. 318–323. URL http://ieeexplore.ieee.org/xpls/abs{_}all.jsp?arnumber=6693856.

[18] Mitchell, I. M., "Application of Levle Set Methods to Control and Reachability Problems in Continuous and Hybrid Systems," Ph.D. thesis, Stanford University, 2002.

[19] Kaynama, S., "Scalable Techniques for the Computation of Viable and Reachable Sets," Ph.D. thesis, 2012. URL https://circle.ubc.ca/bitstream/id/163221/ubc{_}2012{_}fall{_}kaynama{_}shahab.pdf.

[20] Zhang, Y., de Visser, C. C., and Chu, Q. P., "Aircraft Damage Identification and Classification for Database-driven Online Safe Flight Envelope Prediction," *AIAA Atmospheric Flight Mechanics Conference*, 2017, pp. 1–11. doi:10.2514/6.2016-2011, URL http://arc.aiaa.org/doi/10.2514/6.2016-2011.

[21] Mulder, J. A., Sridhar, J. K., and Breeman., J. H., *Identification of Dynamic Systems-Applications to Aircraft Part 2: Nonlinear Analysis and Manoeuvre Design.*, Vol. 3, North Atlantic Treaty Organization, Advisory Group for Aerospace Research and Development., 1995.

[22] Lopez, I., and Sarigul-Klijn, N., "A Review of Uncertainty in Flight Vehicle Structural Damage Monitoring, Diagnosis and Control: Challenges and Opportunities," *Progress in Aerospace Sciences*, Vol. 46, No. 7, 2010, pp. 247–273. doi:10.1016/j.paerosci.2010.03.003.

[23] Moncayo, H., Perhinschi, M. G., and Davis, J., "Artificial-Immune-System-Based Aircraft Failure Evaluation over Extended Flight Envelope," *Journal of Guidance, Control, and Dynamics*, Vol. 34, No. 4, 2011, pp. 989–1001. doi:10.2514/1.52748, URL http://arc.aiaa.org/doi/abs/10.2514/1.52748.

[24] Lombaerts, T., Huisman, H., Chu, Q. P., Mulder, J., and Joosten, D., "Nonlinear Reconfiguring Flight Control Based on Online Physical Model Identification," *Journal of Guidance, Control, and Dynamics*, Vol. 32, No. 3, 2009, pp. 727–748. doi:10.2514/1.40788.

[25] Tang, L., Roemer, M., Bharadwaj, S., and Belcastro, C., "An Integrated Health Assessment and Fault Contingency Management System for Aircraft," *AIAA Guidance Navigation and Control Conference*, 2008.

[26] Carl S. Byington, P. S., "A Model-Based Approach to Prognostics and Health Management for Flight Control Actuators," *IEEE Aerospace Conference Proceedings*, 2004.

[27] Lombaerts, T., Schuet, S., Acosta, D., and Kaneshige, J., "On-Line Safe Flight Envelope Determination for Impaired Aircraft," *Advances in Aerospace Guidance, Navigation and Control*, 2015, pp. 263–282. doi:10.1007/978-3-319-17518-8, URL http://link.springer.com/10.1007/978-3-319-17518-8.

[28] Belcastro, F. J. V., Christine M., "Aircraft Loss-of-Control Accident Analysis," *AIAA Guidance, Navigation and Control Conference*, 2010.

[29] Shah, G., "Aerodynamic Effects and Modeling of Damage to Transport Aircraft," *AIAA Guidance, Navigation and Control Conference and Exhibit*, 2008. URL http://arc.aiaa.org/doi/pdf/10.2514/6.2008-6203.

[30] Oishi, M., Mitchell, I. M., Tomlin, C., and Saint-Pierre, P., "Computing Viable Sets and Reachable Sets to Design Feedback Linearizing Control Laws Under Saturation," *Proceedings of the 45th IEEE Conference on Decision and Control*, 2006, pp. 3801–3807. doi:10.1109/CDC.2006.377614.

[31] Gillula, J. H., Hoffmann, G. M., Haomiao Huang, Vitus, M. P., and Tomlin, C., "Applications of Hybrid Reachability Analysis to Robotic Aerial Vehicles," *The International Journal of Robotics Research*, Vol. 30, No. 3, 2011, pp. 335–354. doi:10.1177/0278364910387173.

[32] Mitchell, I. M., "Comparing Forward and Backward Reachability as Tools for Safety Analysis," *Hybrid systems: computation and control*, edited by A. Bemporad, A. Bicchi, and G. Buttazzo, Springer Berlin Heidelberg, 2007, pp. 428–443. doi:10.1007/978-3-540-71493-4{_}34.

[33] Fedkiw, S., *Level Set Methods and Dynamic Implicit Surfaces*, Vol. 153, Springer, 2003. URL http://link.springer.com/content/pdf/10.1007/b98879.pdf.

[34] Mitchell, I. M., "A Toolbox of Level Set Methods (Version 1.1)," Tech. rep., 2007.

[35] Tomlin, C., Lygeros, J., and Sastry, S., "A Game Theoretic Approach to Controller Design for Hybrid Systems," *Proceedings of the IEEE*, Vol. 88, No. 7, 2000. doi:10.1109/5.871303.

[36] Lombaerts, T., Schuet, S., and Wheeler, K., "Safe Maneuvering Envelope Estimation Based on A Physical Approach," *Guidance, Navigation, and Control and Co-located Conferences*, 2013. URL http://arc.aiaa.org/doi/pdf/10.2514/6.2013-4618.

[37] Lombaerts, T., Schuet, S., Acosta, D., and Kaneshige, J. T., "Piloted Simulator Evaluation of Maneuvering Envelope Information for Flight Crew Awareness," *arc.aiaa.org*, 2015. URL http://arc.aiaa.org/doi/pdf/10.2514/6.2015-1546.

[38] Bayen, A. M., Mitchell, I. M., Oishi, M., and Tomlin, C., "Aircraft Autolander Safety Analysis Through Optimal Control-Based Reach Set Computation," *Journal of Guidance, Control, and Dynamics*, Vol. 30, No. 1, 2007, pp. 68–77. doi:10.2514/1.21562, URL http://arc.aiaa.org/doi/abs/10.2514/1.21562.

[39] Shah, G., Foster, J., and Cunningham, K., "Simulation Modeling for Off-Norminal Conditions-Where Are We Now?" *AIAA Modeling and Simulation Technologies Conference*, Toronto, 2010.

[40] Stevens, B., and Lewis, F., *Aircraft control and simulation*, Wiley, 1992.

[41] Shah, G., and Hill, M., "Flight Dynamics Modeling and Simulation of a Damaged Transport Aircraft," *AIAA Modeling and Simulation Technologies*, 2012. URL http://arc.aiaa.org/doi/pdf/10.2514/6.2012-4632.

[42] Cunningham, K., Cox, D., Murri, D., and Riddick, S., "A Piloted Evaluation of Damage Accommodating Flight Control Using a Remotely Piloted Vehicle," *AIAA Guidance, Navigation, and Control Conference*, 2011. doi:10.2514/6.2011-6451, URL http://arc.aiaa.org/doi/10.2514/6.2011-6451.

[43] Frink, N. T., Murphy, P. C., Atkins, H. L., Viken, S. A., Petrilli, J. L., Gopalarathnam, A., and Paul, R. C., "Computational Aerodynamic Modeling Tools for Aircraft Loss of Control," *Journal of Guidance, Control, and Dynamics*, Vol. 40, No. 4, 2017, pp. 789–803. doi:10.2514/1.G001736, URL https://arc.aiaa.org/doi/10.2514/1.G001736.

[44] NASA, "Flight Dynamics Simulation of a Generic Transport Model," , 2016. Https://software.nasa.gov/software/LAR-17625-1.

[45] Nabi, H. N., "Effects of Structural Failures on the Safe Flight Envelope of Aircraft," Master's thesis, Delft University of Technology, 2016.

[46] Nguyen, N. T., Krishnakumar, K. S., Kaneshige, J. T., and Nespeca, P., "Flight Dynamics and Hybrid Adaptive Control of Damaged Aircraft," *Journal of Guidance, Control, and Dynamics*, Vol. 31, No. 3, 2008, pp. 751–764. doi:10.2514/1.28142, URL http://arc.aiaa.org/doi/abs/10.2514/1.28142.

[47] Boskovic, J. D., Knoebel, N., Mehra, R. K., and Gregory, I., "An Integrated Approach to Damage Accommodation in Flight Control," *AIAA Guidance, Navigation and Control Conference and Exhibit*, 2008.

[48] Cook, M. V., *Flight Dynamics Principles*, 2nd ed., Elsevier, 2013. doi:10.1016/C2010-0-65889-5.

[49] Zhao, H.-k., and Fedkiw, R., "Fast Surface Reconstruction Using the Level Set Method," *Variational and Level Set Methods in Computer Vision*, 2001, pp. 194–201. doi:10.1109/VLSM.2001.938900.

[50] Sethian, J. A., "Evolution, Implementation, and Application of Level Set and Fast Marching Methods for Advancing Fronts," *Journal of Computational Physics*, Vol. 169, No. 2, 2001, pp. 503–555. doi:http://dx.doi.org/10.1006/jcph.2000.6657, URL http://www.sciencedirect.com/science/article/pii/S0021999100966579.

[51] Sethian, J. A., "A Fast Marching Level Set Method for Monotonically Advancing Fronts," *Pnas*, Vol. 93, No. 4, 1996, pp. 1591–1595. doi:10.1073/pnas.93.4.1591.

[52] Adalsteinsson, D., and Sethian, J., "The Fast Construction of Extension Velocities in Level Set Methods," *Journal of Computational Physics*, Vol. 148, No. 1, 1999, pp. 2–22. doi:10.1006/jcph.1998.6090, URL http://www.sciencedirect.com/science/article/pii/S0021999198960909.

[53] Sethian, J. a., "Fast Marching Methods," *SIAM Review*, Vol. 41, No. 2, 1999, pp. 199–235. doi:10.1137/S0036144598347059, URL http://epubs.siam.org/doi/abs/10.1137/S0036144598347059.

[54] Malladi, R., Sethian, J., and Vemuri, B., "Shape Modeling with Front Propagation: A Level Set Approach," *IEEE Transactions on Pattern Analysis and Machine Intelligence*, Vol. 17, No. 2, 1995, pp. 158–175. doi:10.1109/34.368173, URL http://ieeexplore.ieee.org/lpdocs/epic03/wrapper.htm?arnumber=368173.